Hindawi
Geofluids
Volume 2022, Article ID 6728045, 16 pages
https://doi.org/10.1155/2022/6728045

Research Article

Evaluation Method of Water Hazard Control Effect of Coal Seam Floor in Deep Mining: Sequence Verification Evaluation

Yanbo Hu,[1] **Wenping Li**,[2] **Qiqing Wang**,[2] **Xinmin Chen**,[1] **and Gang Zheng**[3]

[1]*School of Transportation Engineering, Nanjing Tech University, Nanjing, 211816 Jiangsu, China*
[2]*School of Resources and Geosciences, China University of Mining and Technology, Xuzhou, 221116 Jiangsu, China*
[3]*China Coal Technology & Engineering Group Xi'an Research Institute, China*

Correspondence should be addressed to Yanbo Hu; hyb@njtech.edu.cn

Received 31 August 2022; Accepted 18 October 2022; Published 29 October 2022

Academic Editor: Yu Wang

Deep, highly pressurized aquifers seriously threaten the exploitation of resources of North China coalfield. At present, there is no particular guidance system to evaluate the prevention and control effect of water inrush disaster in deep coal seam mining. Therefore, this research focuses on the evaluation of the method for confined water disaster prevention and control effect of deep coal seam mining. Based upon various methods, such as effective thickness and water resistance capacity of aquifuge, water inrush coefficient, GIS (Geographic Information System) analysis of grouting data, dense drilling verification, and professional analysis system based on integrated sequence evaluation, the evaluation of the method for confined water disaster prevention and control effect of deep coal seam mining was put forward for the first time. The proposed method was called the "sequence verification evaluation (SVE)" method. The prevention and control of the effects of Ordovician water inrush disaster in deep mining of Huanghebei coalfield was evaluated using the proposed SVE method. The results show that the SVE method can effectively reflect the prevention and control of the effects of water inrush from confined water and provide scientific basis for the safe production of deep coal seam mining.

1. Introduction

Since becoming the "People's Republic," coal resources have become the main driving force for China's economic development. In recent years, with the increase in the depth of mining for coal resources, especially, the mining areas in the middle and eastern parts of China have basically entered the deep mining mode [1]. The increase in mining depth has brought great challenges to safe operations of coal mines. In particular, the threat of confined water in deep coal seam floor has seriously affected the safe operation of mines for the exploitation of deep resources [2, 3]. At present, global treatment of water hazard in the deep coal seam floor mainly includes the methods of drainage and pressure reduction, mining under pressure, curtain grouting, and regional grouting transformation. These methods can basically meet the treatment of pressure water hazard in deep coal seam [4–6]. However, according to some recent statistics, the hazard from water inrush in deep coal seam floor is still on the rise. In this regard, there are two main challenges. The first is that the governance plan was not correct. The governance measures were not in place, and there was a phenomenon of governance in blind areas. Secondly, the evaluation of the method for confined water disaster prevention and control effect of deep coal seam mining is unscientific, which leads to a large deviation in safety evaluations of deep coal seam mining.

In recent years, two research methods have mainly been used for evaluating the prevention and control effect of floor water hazard in deep coal seam mining. First is the calculation of the effectiveness of the water-resisting layer of coal floor using analytical calculations or computer-aided algorithm. In the second approach, the method is verified by analogy of regional coalfield geological conditions combined with geophysical prospecting [7]. At present, the main methods to evaluate the prospects of water disaster in the deep coal seam floor include numerical simulations, vulnerability index method, cusp catastrophe model, water inrush

probability index method, water inrush coefficient-unit water inflow method, logging hydraulic conductivity verification method, water-resisting performance evaluation method of water-resisting layer, mining electricity method, and drilling test verification [8–12]. Moreover, there is no systematic standard to verify the evaluation of the method for confined water disaster prevention and control effect of deep coal seam mining. The main problem is that the geological conditions of deep mining areas are different [13–17]. Therefore, the schemes for preventing and controlling water disasters are also different in these mining areas. Additionally, there are blind spots in the evaluation results, which make it impossible to qualitatively and quantitatively evaluate the control effect strategy.

Therefore, according to the current situation of water disaster prevention and evaluation technology in deep coal seam mining, a novel "sequence verification evaluation (SVE)" method is put forward for the first time, which can make scientific and effective evaluation of the safe mining operation under different regional geological conditions. The practice shows that the evaluation method has the characteristics of high safety and strong operability in evaluating the water inrush in deep coal seam floors. The method can provide reference for the treatment of floor water disaster in deep coal seam mining and has important research and practical significance.

2. Research Area

The QJ coal mine in Huanghebei coalfield is located at the junction of Qihe County and Dong'e County in Dezhou city, Shandong province, China. The mining area is 36.14 km^2, with an approved mining elevation of +30 m-900 m and a designed production capacity of 450 kt/a. Coal seams No. 7, No. 10, No. 11, and No. 13 are available for mining, with reserves of 237.21 million tons. By the end of 2018, the mining of coal seams No. 7 and No. 10 has been completed, and the mining of coal seam No. 11 is threatened by the underlying Xujiazhuang limestone and Ordovician limestone karst-confined water. Due to these risks, the safe operation of the mines was in jeopardy. In order to realize continuous normal production of the mine, it was decided to carry out grouting treatment on the floor water damage of the initial mining in coal seam No. 11 by using the "regional governance mode of water filling aquifer and water conducting structure (RGM)."

As shown in Figure 1, the average thickness of Xujiazhuang limestone under No. 11 coal seam is 12.85 m, 35.52 m away from No. 11 coal seam, with medium water yield, developed karst fissures, abundant water supply, difficult to drain, and large shallow hydraulic conductivity. The average distance between the Xujiazhuang limestone and the Ordovician limestone was about 8 m, which is closely related to Ordovician limestone due to the small distance or dislocation of faults between the Xujiazhuang limestone and the Ordovician limestone.

The thickness of Ordovician limestone area was about 700 m, and the unit water inflow was 0.0204-4.141 L/(s·m), which is confined water of karst fissure, and the water inflow varied significantly from weak to strong. Ordovician limestone supplied water to Xujiazhuang limestone aquifer transversely and longitudinally through fault, which is a strong indirect water-filled aquifer mined in coal seam No. 11.

2.1. General Situation of 1101 Coalface in Coal Seam No. 11. The elevation of 1101 coalface was -339~ -422 m, whereas the width of coalface was 100 m. Moreover, the length was 924 m, and the area was 9.24×10^4 m^2. The average thickness of coal seam was 2.11 m, while the average dip angle of coal seam was 5°. The estimated recoverable reserves of the coalface were 2.496×10^5 T, as shown in Figure 2.

The coal seam of 1101 coalface was in the east-west direction. According to the analysis of prevalent geological conditions during the construction of auxiliary roadway in the coalface, the geological structure of the coalface was found to be simple, and the adjusted mining area of the coalface exhibited two normal faults, as shown by the results presented in Table 1.

2.2. Prevention and Control of Limestone Aquifer. The floor water disaster in the first mining area of coal seam No. 11 in QJ coal mine was controlled by the ground-controlled directional drilling grouting technology (GCDD). Based upon comprehensive consideration of fault, fold axis trace, grouting target layer tendency, interlayer structural plane, maximum horizontal stress direction, and original rock hydrodynamic field direction of the reformed layer, the zoning optimization diagram of grouting drilling track along the layer was obtained. Meanwhile, the grouting hole spacing of Xujiazhuang limestone aquifer was determined by combining the following seven factors: (1) the grouting numerical simulation data of the RFPA 2D simulation system, (2) the maximum spacing of branch holes should not exceed twice the diffusion radius of slurry, (3) drilling should cover the whole processing area as much as possible, (4) the degree of development of Karst of Xujiazhuang limestone aquifer in the first mining area of coal seam No. 11, (5) there are concealed structures, (6) large amount of Ordovician limestone water supply and efficient utilization of horizontal drilling need to be considered, and (7) economically feasible. The drilling arrangement and the implementation scheme of Xujiazhuang limestone prevention in the first mining area of coal seam No. 11 in QJ coal mine are shown in Figure 3.

In order to realize the continuity of normal production in QJ coal mine and reduce the economic risk of grouting reconstruction project, the water disaster control project in the first mining area of coal seam No. 11 was mainly divided into two stages. In the first stage, an area for transforming Xujiazhuang limestone aquifer was delineated, and some of the resources of coal seam No. 11 were rapidly liberated. The feasibility of using "RGM" technology has been verified through the implementation of safe mining. Meanwhile, for the sake of safe mining, the second stage was to select a large area in the first mining area of coal seam No. 11 for Xujiazhuang limestone aquifer's reconstruction project and liberate the remaining resources of coal seam No. 11 in the west wing mining area.

STRATUM	GEOLOGIC COLUMN (1: 500)	THICKNESS (m)	DISTANCE TO 11# (m)
LIMESTONE NO. 4		5.13	3.15
MUDSTONE		1.14	2.01
LIMESTONE NO. 4		2.01	
NO. 11 COAL SEAM		1.86–2.45 / 2.02	
SILTSTONE		5.56	
NO. 13 COAL SEAM		3.18–4.8 / 3.78	5.56
CLAYSTONE		2.53	9.34
SILTSTONE		2.89	11.87
NO. 14 COAL SEAM		0.34	14.76
SILTSTONE		8.96	15.10
MUDSTONE		10.67	24.06
XUJIAZHUANG LIMESTONE		9.87 – 22.32 / 12.85	34.73
CLAYSTONE		9.50	47.58
ORDOVICIAN LIMESTONE		> 700	57.08

Figure 1: Comprehensive histogram of the first mining area of the research mining area.

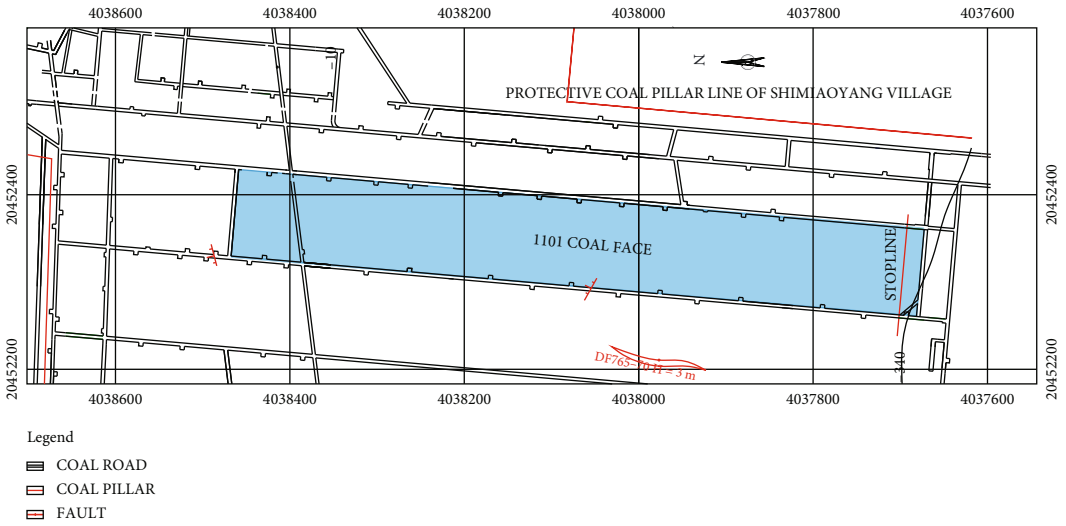

Figure 2: Location map of 1101 coalface.

Table 1: Fault data of the 1101 coalface.

Fault number	Strike	Dip	Properties	Fault throw	Influence degree
F5	81°	40°	Normal fault	1.2 m	Less
F7	65°	50°	Normal fault	0.6 m	Less

Xujiazhuang limestone aquifer is reformed by combining the ground high pressure grouting with auxiliary grouting in underground coalface. According to the sequence of prevention and control, the first mining area was further divided into four areas, as shown in Figure 3. Area I was mainly covered by boreholes (denoted by S1, S3, S6, D1, D6, and D13). Area II was mainly covered by S2, S6, S11, D1, D2, and D6 boreholes. Area III was mainly covered by D8 test hole. D13 borehole was mainly used for regional coverage in the reconstruction area IV.

The water disaster prevention and control project of limestone in the first mining area of coal seam No. 11 started in July, 2016. Up till December 2019, 34 groups of drilling holes had been built and included 21 groups of No. 4 and No. 5 limestone drilling holes and 13 groups of Xujiazhuang limestone drilling holes. The total footage was 96.10 km, with 521 kt of cement and 40 kt of fly ash injected. The prevention and control area was about 1.07 km^2 (including 1102, 1101, 1103, and 1105 coalfaces). Nearly 2.4 million tons of geological reserves were released from coal seam No. 11.

3. Methodology

In this paper, a five-step "SVE" method was proposed to evaluate the effect of the reconstructed layer. The "SVE" method mainly analyzes the hydraulic conductivity, permeable rate, and maximum water resistance coefficient of the target layer of group transformation. Meanwhile, the comprehensive "SVE" method that includes various analyses, such as secondary electrical detection, GIS system analysis of grouting data, and intensive exploration borehole, was adopted. The steps of the "SVE" method are as follows. Firstly, the hydraulic conductivity and permeable rate of the deep coal seam floor aquifer were verified after transformation according to the packer permeability test (PPT). A qualitative evaluation of the treatment effect was conducted within the coalface range. Secondly, the water blocking capacity of the deep coal seam floor aquiclude was evaluated qualitatively. Thirdly, the mine electrical method was used to carry out quantitative detection and analysis of the whole coalface. By comparing the contour slice of low-resistance abnormal area before and after the treatment, the abnormal area after the treatment was determined, and the data about the quantitative abnormal area were summarized. Fourthly, according to the data of single-hole grouting quantity and final grouting pressure, the GIS system was used to quantitatively analyze the abnormal area after the treatment. Fifthly, according to the qualitative and quantitative data obtained from the above four steps, the abnormal area map after the prevention and control of Xujiazhuang limestone aquifer was delineated. After that, the final detection was carried out using intensive detection boreholes in the coalface. Finally, the zoning map of water disaster control effect of deep coal seam floor and the single-hole water inflow data of intensive detection borehole after transformation were obtained. According to the data provided by the "SVE" method, supplementary grouting transformation could be carried out underground or on the ground. After the supplementary transformation, the fifth step was adopted for verification until the water inflow of a single hole became less than the set safety threshold, which meets the mining conditions. The flow chart of the "SVE" system of coal seam floor water disaster control effect is shown in Figure 4.

3.1. Evaluation of Hydraulic Conductivity and Permeable Rate. PPT is an in situ permeability test that determines the permeability characteristics of rock mass according to the relationship between pressure and flow rate. In order to test the effect of grouting reinforcement on the deep coal seam floor, the permeabilities of the target layer and its upper and lower composite layers were tested after the comprehensive grouting reinforcement of the coalface floor was completed. Drilling holes were set up in the auxiliary roadway of the coalface, and the PPT was carried out. The infiltration water volume and final pressure were obtained as the basic data for the evaluation of the reinforcement effect of the deep coal seam floor [18].

3.1.1. Test Method of Drilling Water Pressure Test for Grouting Effect of Floor. The in situ test was carried out according to the code for water pressure test in borehole for water resources and hydropower engineering that was formulated according to the power industry standard of the People's Republic of China (the drilling type of water pressure test is complete penetration of well).

3.1.2. Analytical Method of PPT Data. PPT can effectively measure the unit water absorption rate of fractured rock mass and calculate the hydraulic conductivity and permeable rate of the reformed stratum, thus qualitatively determining the transformation effect of limestone aquifer.

Unit water absorption is the index of rock mass permeability, which refers to the water absorption per unit time of the test section per unit length under the height of unit head. It is calculated as

$$\omega = \frac{Q}{H \cdot L}, \tag{1}$$

where ω is the unit water absorption (L/min m m), Q is the pressure water flow rate at steady state (L/min), H is the height of water head during the test (m), and L is the length of PPT section (m).

Calculation of hydraulic conductivity of rock mass is as follows:

$$K_1 = 0.525 \cdot \omega \cdot \lg\frac{0.66 \cdot L}{r}, \tag{2}$$

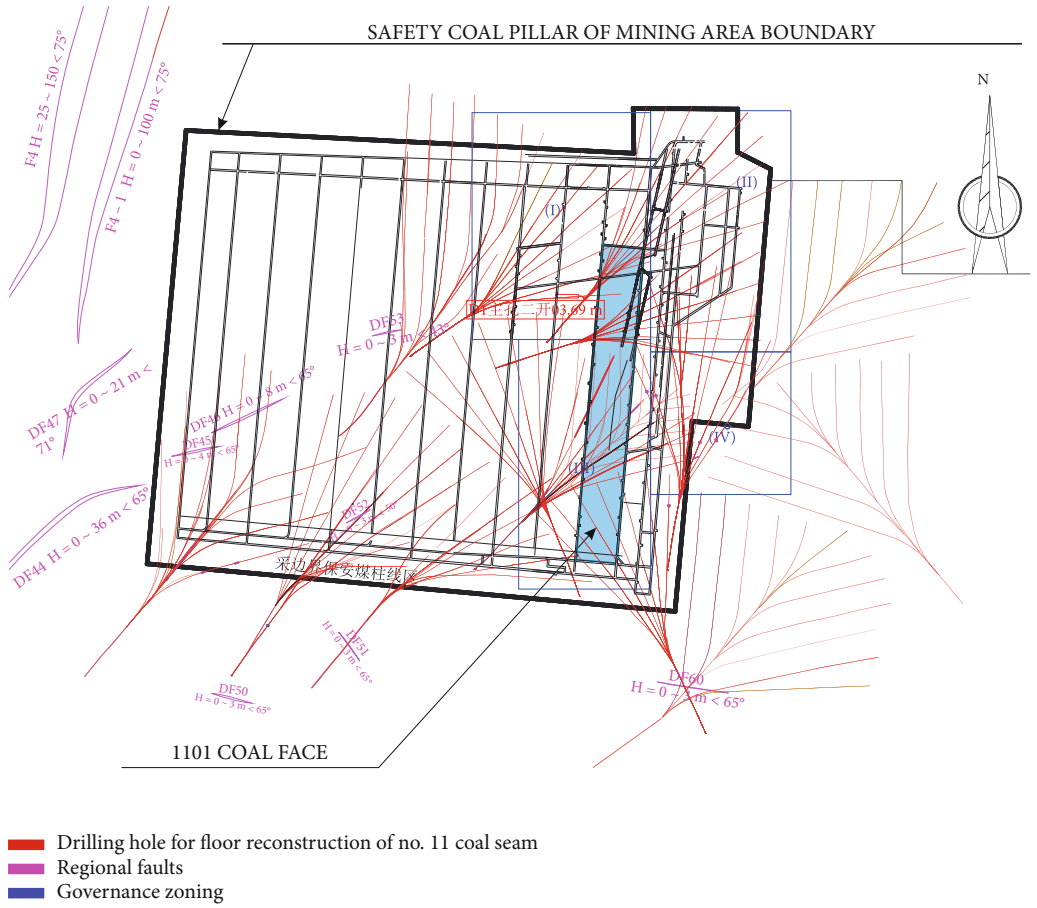

Figure 3: Layout of directional drilling and grouting in Xujiazhuang limestone aquifer.

$$K_2 = 0.525 \cdot \omega \cdot \lg \frac{1.32 \cdot L}{r}, \tag{3}$$

where r is the radius of PPT borehole (m) and K is the hydraulic conductivity.

According to Equations (2) and (3), when the thickness of water-resisting layer under coal seam is larger than the length of the test section, the hydraulic conductivity of the rock mass is calculated by Equation (2). On the other hand, when the thickness of the water-resisting layer under coal seam is less than the length of the test section, Equation (3) is used to calculate the hydraulic conductivity of the rock mass.

Calculation of the permeable rate is as follows:

$$q = \frac{Q}{P \cdot L}, \tag{4}$$

where$P$is the water pressure value (MPa) and q is the permeable rate (Lu).

Finally, according to the national standard of People's Republic of China ("Code for Geological Investigation of Water Conservancy and Hydropower Engineering"), the permeability classification standard of rock and soil mass is presented in Table 2. When the hydraulic conductivity of rock mass was $10-6 \le K < 10-5$ and the permeable rate was $0.1 \le q < 1$, the permeability grade was micropermeable, which indicates that the floor rock was transformed into micropermeable rock mass after grouting reinforcement. Moreover, the rock mass had good water resistance performance (Equation (4)).

3.2. Evaluation of the Water Blocking Capability of Coal Seam Floor. The water resistance coefficient of floor rock in deep coal seam is an index reflecting the average water resistance of floor aquiclude. In the risk assessment of water inrush from deep coal seam floor, the water resistance coefficient is an important parameter to calculate the effective thickness of the water resisting layer of the coal seam floor. The calculation of water inrush coefficient of the deep coal seam floor is an important method for qualitative evaluation of the effect of floor grouting reinforcement.

In order to calculate the diffusion radius of the injected pressurized water, the diffusion path of water injection should first be considered. Generally, under the action of pressure, water will move along the layers of rock and rock fissures. This means that water will permeate along the fissures with low rock resistance, and the seepage speed will generally be low. Under such conditions, the flow can be considered Newtonian flow. However, under the action of high-pressure water, the pressurized water will split the surrounding rock of the borehole. If there is a weak layer in the rock formation, the water will first penetrate along the weak layer.

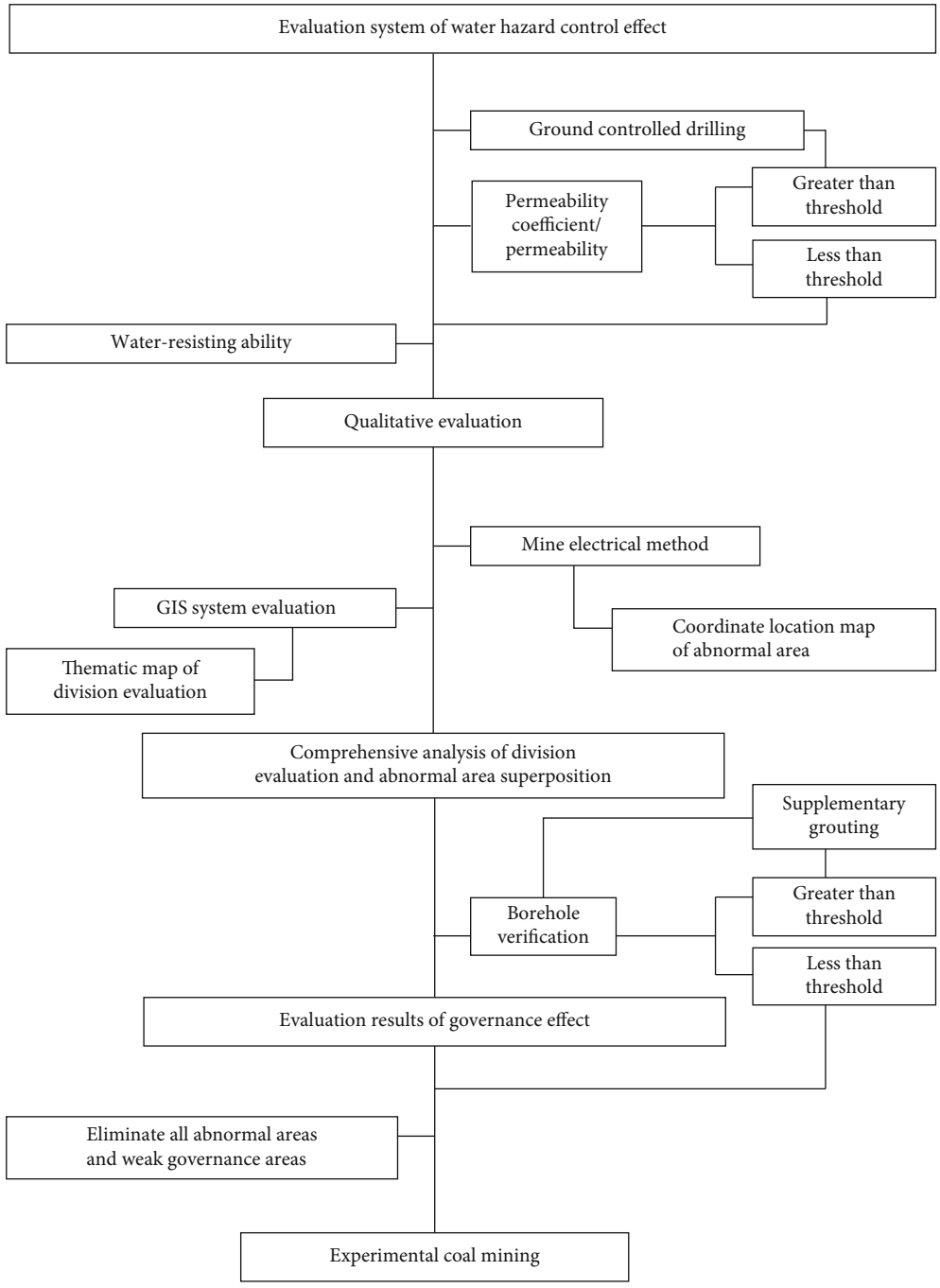

Figure 4: Flow chart of the "SVE" system for water hazard control effect of deep coal seam floor.

Secondly, the head loss should be considered. According to a previous work, due to the existence of viscosity coefficient, there is a certain head loss in the flow of liquid, and the main forms of loss are along-the-way loss and local head loss [19].

The along-the-way head loss is the energy loss caused by the work done to overcome frictional resistance. During the injection of water, the actual driving will reduce the seepage pressure. Moreover, seepage resistance is the frictional force between hydrostatic pressure and the material filling the rock fissures. Therefore, with the increase of permeability distance, both the water pressure in the fracture and the permeability of water will gradually decrease. Until the hydrostatic pressure and water injection pressure in the fissure tend to be balanced, the water head stops the seepage, and the diffusion radius reaches the maximum value.

3.2.1. Calculation Model of Pressurized Water Diffusion Radius. According to the above analysis, the calculation model of the diffusion radius of pressurized water is established and is as follows. (1) It is assumed that the seepage velocity of water is small. Therefore, the change in velocity

Table 2: Classification standard for permeability of rock and soil.

Permeability grade	Hydraulic conductivity, K (cm/s)	Permeable rate, q (Lu)	Rock mass characteristics
Infinitesimal permeability	$K < 10^{-6}$	$q < 0.1$	Complete rock mass or fractured rock mass with equivalent opening less than 0.025 mm
Micropermeability	$10^{-6} \le K < 10^{-5}$	$0.1 \le q < 1$	Rock mass with equivalent opening of 0.025 mm-0.05 mm fractures
Weak permeability	$10^{-5} \le K < 10^{-4}$	$1 \le q < 10$	Rock mass with equivalent opening of 0.05 mm-0.01 mm fractures
Medium permeability	$10^{-4} \le K < 10^{-2}$	$10 \le q < 100$	Rock mass with equivalent opening of 0.01 mm-0.5 mm fractures
High permeability	$10^{-2} \le K < 100$	$q \ge 100$	Rock mass with equivalent opening of 0.5 mm-2.5 mm fractures
Strong permeability	$K \ge 100$		A fractured rock mass with communicating holes or equivalent openings larger than 2.5 mm

is also small, which is in accordance with Newtonian flow. (2) In addition to the partial pressure loss in fracturing and filling cracks, the remaining water pressure is mainly to overcome the resistance of water flowing in rock cracks. With the increase in penetration distance, the water pressure in the fracture gradually decreases. Accordingly, this results in a decrease in water's permeability. After the water pressure and water injection pressure in the fracture acquire equilibrium, the diffusion radius reaches the maximum value. (3) The model ignores the inhomogeneity of the distribution of stress stratum, and its diffusion radius is a circular diffusion surface with the water pressure hole as the center for plane radial radiation. According to these conditions, the pressurized water radiation surface is calculated as a point source spherical model, as shown in Figure 5.

In Figure 5, P_c is the injection pressure, P_1 is the attenuation pressure distributed along the fracture, r is the diffusion radius of water, R is the maximum diffusion radius of water, r_c is the radius of water injection borehole, and P_0 is the hydrostatic pressure. Although the model ignores the disorder of water flow in rock mass, the heterogeneity of rock fracture, and the in situ stress distribution, it is similar to the actual state of pressurized water injection. The model is more convenient for analyzing the diffusion pattern of pressurized water injection and the attenuation pattern of water pressure along fractures.

3.2.2. Calculation of Water Injection Diffusion Radius. The Navier-Stokes equation should be satisfied if the water body flows along the X fracture surface:

$$\frac{\partial u}{\partial t} + u\frac{\partial u}{\partial x} = f_x - \frac{1}{\rho}\frac{\partial p}{\partial x} + v\Delta u\frac{\partial u}{\partial t} + u\frac{\partial u}{\partial x}, \tag{5}$$

where u is the velocity of the water body, f is the mass force, ρ is the density of fluid, v is the kinematic viscosity of fluid, and p is the grouting pressure.

Because of the small change of permeability velocity, the change in viscosity can be neglected. Therefore, the Poiseuille solution is given by the following equations.

$$V = -\frac{h^2}{3\mu}\cdot\frac{dp}{dx} = \frac{h^2}{3\mu}\cdot\frac{\Delta P}{L}, \tag{6}$$

$$\mu = \frac{0.01775}{1 + 0.0337t + 0.000221t^2}, \tag{7}$$

where V is the average speed; μ is the viscosity coefficient of the fluid's movement, which depends on water temperature; h is the half gap width of rock layer, where $h = b/2$; and b is the total fracture width of rock layer, which is the product of total thickness (H) and fracture rate (n) of the fractured rock layer in the pressure hole (the fracture rate (n) is generally between 1 and 2%). When the injection pressure is small and the amount of injected water is large, the fracture rate of the water pressure hole layer is large. When the injection pressure is high and the injected water's volume is small, the fracture rate of the water pressure hole layer is low, and ΔP is the pressure difference.

Under the action of water injection pressure (P_c), the water flows out from the water injection hole with radius r_c and radiates around along the direction of the plane of fracture. The relationship between the water flow, flow velocity, and fracture width is given by the following equation:

$$Q = 4\pi r \cdot hV, \tag{8}$$

where Q is the steady flow of pressurized water.

According to the boundary condition ($\begin{cases} r = r_c : P = P_c \\ r = R : P = P_0 \end{cases}$), Equation (6) is replaced by Equation (8) for integration, and Equations (9) and (10) are obtained.

$$P = P_C - \frac{6\mu Q}{\pi b^3}\ln\frac{r}{r_c}, \tag{9}$$

$$\ln\frac{R}{r_c} = \frac{\Delta P\pi b^3}{6Q\mu}. \tag{10}$$

According to Equation (10), the maximum diffusion

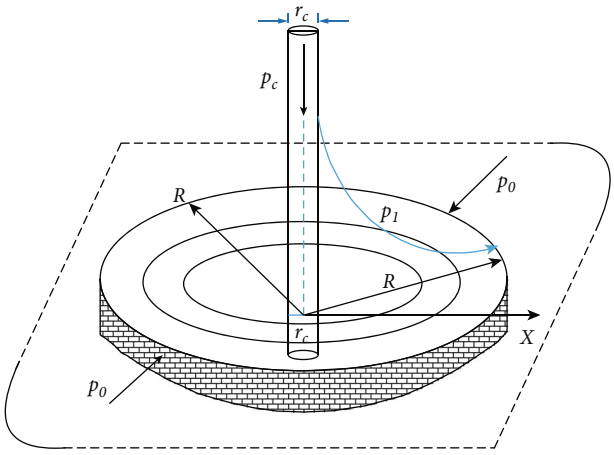

Figure 5: Schematic of the calculation model for diffusion radius of pressurized water.

radius (R) of water injection in the reformed formation can be obtained.

3.2.3. Calculation of the Maximum Water-Blocking Coefficient and Critical Water Inrush Coefficient of Rock Mass after the Floor Grouting Transformation of Coalface

(1) Calculation of Water Resistance Coefficient after Grouting Transformation and Reinforcement. The water resistance coefficient refers to the water resistance pressure of the rock mass per unit thickness. Therefore, according to the maximum diffusion radius of water injection, the water resistance coefficient of the floor rock mass covered by the detection hole is calculated using

$$Z_{\max} = \frac{P_c}{R}, \tag{11}$$

where P_c is the injection water pressure (MPa) and R is the maximum diffusion radius (m).

(2) Calculation of Critical Water Inrush Coefficient of the Floor of Coalface after Grouting Reinforcement. Equation (12) holds when the working face floor is in critical water inrush state.

$$T_0 = Z_{\max}. \tag{12}$$

The conventional calculation method of water inrush coefficient of coalface floor is given by

$$T_s = \frac{P}{M - C}, \tag{13}$$

where T_s is the water inrush coefficient of the coalface floor (MPa/m), M is the aquiclude thickness of the coalface floor (m), and C is the maximum failure depth of the coalface floor (m).

Therefore, when the actual water inrush coefficient is greater than the critical water inrush coefficient, it is predicted that the coalface is in water inrush state. When the actual water inrush coefficient is smaller than the critical water inrush coefficient, the coalface is predicted to be in a safe state.

3.3. Evaluation of Mine Electrical Method. In the process of water disaster control of the deep coal seam floor, the change of apparent resistivity in the coal seam floor can be measured using electrical exploration. The apparent resistivity is closely related to the water-bearing property of rock stratum. This means that, when the water-rich is strong, the apparent resistivity is low. However, when the water-rich is weak, the apparent resistivity is high. The limestone aquifer under the floor of deep coal seam is generally a high-resistivity layer; however, the apparent resistivity is low during local karst development. Therefore, the abnormal area with low apparent resistivity is generally a water-bearing abnormal area. After grouting transformation of coal seam floor rock, limestone fracture is basically filled with slurry, and the apparent resistivity of limestone layer will increase. Therefore, after grouting transformation, the deep coal seam floor can be tested in situ using the mine electricity method, and the effect of grouting transformation can be judged according to the apparent resistivity of coal seam floor rock [20].

3.4. Evaluation of Water Disaster Control Effect Based on GIS. Two important grouting indices are the final pressure and final quantity of single-point grouting in branch drilling. According to the regional coordinate statistics of grouting transformation, the final grouting pressure for each coordinate point is recorded. The surfer system is used to locate the regional grouting, whereas the Kriging algorithm is used to calculate the interpolation. Furthermore, the final pressure of single-point grouting is segmented. Generally, the standard zone, qualified zone, and weak zone (or relatively weak zone) can be set to determine the interval of the final pressure of each section. The data generated by the surfer system can be imported into the GIS system for further processing.

Optimization of the spacing of horizontal boreholes results in a fixed value, and only the boundary problem of the outermost horizontal boreholes needs to be considered in the GIS system. Under normal circumstances, the grouting pressure of horizontal drilling holes shall not be less than 2 times the water pressure of the reformed layer. Additionally, as the qualified grouting pressure of horizontal branch drilling holes, the ground high-pressure grouting equipment shall be stabilized in a low gear for 30 minutes. This is done to obtain the partition map of grouting final pressure effect in the whole reconstruction area. After that, the single-point grouting data in the weak area or relatively weak area is used to calculate the single-point grouting data in the area and conduct comprehensive analysis to determine the overall grouting transformation effect.

3.5. Evaluation Using Dense Boreholes. For the water disaster of the deep coal seam floor, the most intuitive and effective method to evaluate the effect of grouting to transform the

thin limestone aquifer on the floor is to arrange the drilling holes in the underground transformation layer and measure the water inflow of a single hole. In order to effectively detect the grouting effect of large-area ground directional drilling in the area after grouting transformation, it is necessary to design the location and spacing of underground exploration drilling holes according to the size of the transformation area. Under normal circumstances, the final spacing of underground construction exploration drilling holes should not be greater than 2 times the spacing of bedding grouting drilling holes. The distance between the inspection holes in the underground construction at the bottom of the hole is generally less than 2 times the distance between the horizontal holes. Secondly, it is necessary to set the bottom position of the inspection hole. Under normal circumstances, the bottom position of the hole generally covers half of the thickness of the grouting transformation layer. Finally, the threshold should be set to analyze the water inflow of the inspection borehole.

In view of the water inflow of the single hole of the deep coal seam floor grouting transformation layer in the eastern mining area of North China type coalfield, the water inflow of the single hole is generally set to be no more than $5\,m^3/h$ (if the working face passes through the fault location, additional measures shall be taken for evaluation and analysis).

3.6. Sequence Verification Evaluation Method. In short, the sequence verification system is composed of hydraulic conductivity analysis, permeable rate analysis, maximum water blocking coefficient analysis, secondary electricity analysis, GIS system analysis, intensive inspection, and drilling analysis and comprehensively evaluates the treatment effect of floor water disaster in deep coal mine area in the eastern margin of North China. The method consists of the following main steps. (1) The PPT was carried out on the thin limestone aquifer of the reformed deep coal seam floor. According to the specific mining face area to be evaluated, test drilling holes are constructed in the auxiliary tunnel of the coalface. Generally, the spacing of the PPT boreholes is not more than 300 m, which is determined according to the design of coalface. According to the test results, the hydraulic conductivity and permeable rate of the grouting-modified layer are calculated by sections. According to the permeability classification standard of rock and soil in "code for geological investigation of water conservancy and Hydropower Engineering," the coalface is divided into various zones, and the permeability zoning map is obtained. (2) The maximum water resistance coefficient of the test area is converted using the PPT data. By comparing the maximum water resistance coefficient of each region with the actual water inrush coefficient, the regions where the actual water inrush coefficient is greater than or equal to the maximum water resistance coefficient can be classified. (3) Based upon the mine electrical method for in situ testing of the floor rock layer of the coal mining face, the effect of grouting transformation is adjudged according to the apparent resistivity of the coal seam floor rock, and the low-resistance abnormal profile of the apparent resistivity is obtained. (4) The integrated pressure of GCDD single-point coordinate position is analyzed using GIS, and the completed area is partitioned by setting a threshold value, so that the weak area or relatively weak area of grouting transformation is obtained. (5) Large-scale exploration is carried out by using dense holes. According to the design scheme of inspection drilling hole and the threshold value of water inflow from a single hole, the grouting area that does not meet the design requirements can be obtained. Based upon the obtained results, the evaluation of grouting reform effect of the deep coal seam floor is conducted.

3.7. Comparative Analysis. As mentioned above, up till now, there is no relatively perfect evaluation method for the prevention and control effects of water inrush disaster in deep mining at home and abroad. The proposed SVE method is based on each individual evaluation method, seeking advantages of the individual methods and avoiding their disadvantages. Furthermore, the SVE method makes use of the geographic information system and forms an evaluation method that can carry out qualitative and quantitative analysis. Compared with the traditional single evaluation method, the evaluation results are more accurate and have better practical significance.

The SVE method has two parts, namely, the qualitative analysis and the quantitative evaluation. The method can partition the prevention and control effect of regional water inrush disaster, effectively evaluate the prevention and control effect of water hazard at each coordinate point, and provide guidance on the safe production of deep mines.

However, some conventional individual evaluation methods only have the qualitative evaluation, and the specific water hazard threat coordination points cannot be determined. Some examples of such methods include the evaluation method of hydraulic conductivity and permeable rate, evaluation method of water blocking ability of coal seam floor, and water inrush coefficient method. There are still some evaluation methods that can be used for quantitative evaluation, but long-term practice has proved that the quantitative evaluation accuracy of the single evaluation method is not high, and it is also easy to lead to water inrush disasters, such as mine electrical method and underground borehole verification method.

Therefore, the proposed SVE method offers a more concrete scientific basis than the qualitative analysis in the early stage and the quantitative analysis in the later stage. This is due to the reason that the method is composed of various individual methods and benefits from the advantages of individual methods while avoiding their disadvantages.

4. Evaluation of Prevention and Control Effect of Floor Water Damage in 1101 Coalface

4.1. Hydraulic Conductivity and Permeable Rate. According to the technical requirements of the methodology, four boreholes were constructed in the auxiliary roadway of 1101 coalface with spacing of 200 m. After grouting transformation, the PPT of Xujiazhuang limestone was carried out. The experimental results are presented in Table 3.

Table 3: Water pressure test data after grouting transformation of Xujiazhuang limestone aquifer.

No.	Hydraulic pressure (MPa)	Time (min)	Regime flow (L/min)	Drilling radius (m)	Test length (m)
D-1	6	30	39	0.075	25.69
D-2	6	30	28	0.075	35.4
D-3	7	30	35	0.075	36.98
D-4	7	30	52	0.075	38.54

Table 4: Calculation table of specific water absorption, permeable rate, and hydraulic conductivity of Xujiazhuang limestone aquifer after grouting transformation.

No.	Specific water absorption (L/MPa m min)	Permeable rate (Lu)	Hydraulic conductivity (cm/s)
D-1	0.0025	0.2530	5.22*E*-06
D-2	0.0013	0.1318	2.88*E*-06
D-3	0.0014	0.1352	2.98*E*-06
D-4	0.0019	0.1928	4.28*E*-06

The specific water absorption, hydraulic conductivity, and permeable rate of Xujiazhuang limestone aquifer after grouting are calculated using Equations (1), (2), and (4), respectively, and the corresponding results are presented in Table 4.

According to the results presented in Table 4, the hydraulic conductivity of Xujiazhuang limestone under the floor of 1101 coalface of QJ coal mine after grouting transformation lied within the range of $2.88 \times 10^{-6} - 5.22e \times 10^{-6}$ cm/s, while the permeable rate lied within the range of 0.1318-0.2530 Lu. According to the classification standard of rock and soil permeabilities in the code for geological investigation of water conservancy and hydropower engineering, when the hydraulic conductivity of rock mass and the permeable rate were $10^{-6} \le K < 10^{-5}$ cm/s and $0.1 \le q < 1$, respectively, the permeability grade of rock mass was micropermeability, indicating that the Xujiazhuang limestone aquifer was transformed into micropermeable rock mass after the floor grouting reform of 1101 coalface and that it has good water-resisting property at this stage.

4.2. Evaluation of Water-Resisting Ability. According to the proposed methodology, the water-resisting ability of the aquiclude after grouting is evaluated. Firstly, four boreholes were drilled in the auxiliary roadway construction of 1101 coalface, and the core was taken for analysis to test the fissure ratio of the underlying strata of coal seam No. 11. Secondly, according to the PPT data and Equation (10), the maximum diffusion radius of each borehole was calculated. Finally, the maximum diffusion radius was used to calculate the water resistance coefficient of the aquiclude after grouting.

QJ coal mine belongs to the eastern margin of coal-accumulating area in North China and has typical geological characteristics of North China coalfield with Ordovician limestone as the coal measure basement. According to the recent data of Ordovician limestone observation well D5-7, the water level elevation was +29 m. The lowest elevation of 1101 coalface was –422 m, and the distance between coal seam No. 11 and Ordovician limestone was 58.86-74.87 m. If the minimum thickness was 58.86 m, the water pressure borne by the aquiclude was 5.10 MPa. The drilling data of PPT in auxiliary roadway of coalface is presented in Table 5.

According to the results presented in Table 5 and Equation (10), the maximum diffusion radii of the four test boreholes in auxiliary roadway of 1101 coalface are presented in Table 6.

The calculations of maximum water resistance coefficient ($Z_{\max}$) and Ordovician limestone water inrush coefficient (T_0) of 1101 coalface floor grouting transformation are as follows:

(a) Calculation of the water resistance coefficient after grouting and reinforcement of coal seam floor rock stratum is as follows: the water resistance coefficient of rock mass refers to the water blocking pressure of the rock mass per unit thickness. According to Equation (11), the water resistance coefficient of each stratum is calculated, and the corresponding results are presented in Table 7

(b) After grouting and strengthening the floor strata of 1101 coalface, the critical water inrush value (T_0) of Ordovician limestone and the water inrush coefficient (T_s) of the floor of the coalface under conventional mode are calculated

According to Equation (11), when the floor of 1101 coalface is in critical water inrush state, Equation (14) should hold.

$$T_0 = Z_{\max}. \tag{14}$$

Conventionally, the floor water inrush coefficient of 1101 coalface is calculated using

$$T_s = \frac{P}{M - C}. \tag{15}$$

The "air bag solution leak detection method" was used to measure the floor failure depth of 1102 trial mining face, and the results show that it was about 15.6 m. Coalface 1102 is located near coalface 1101. According to the analogy method, Equation (16) is used to determine the result of

Table 5: Data of PPT and core drilling.

No.	Hydraulic pressure (MPa)	Time (min)	Regime flow (L/min)	Drilling radius (m)	Test length (m)	Fracture thickness (m)	Fissure ratio of the test section (%)
D-1	6	30	39	0.075	25.69	18.32	1.58
D-2	6	30	28	0.075	35.4	21.59	1.20
D-3	7	30	35	0.075	36.98	29.81	0.89
D-4	7	30	52	0.075	38.54	24.32	1.25

Table 6: Table of maximum diffusion radius in PPT.

No.	Regime flow (m^3)	Crack width of test section (m)	Dispersion radius (m)
D-1	1.17	0.2895	47.19
D-2	0.84	0.2591	46.82
D-3	1.05	0.2653	47.51
D-4	1.56	0.3040	51.53

Table 7: Table of water resistance coefficient of 1101 coalface floor.

No.	Water injection pressure (MPa)	Dispersion radius (m)	Maximum water resistance coefficient (MPa/m)
D-1	6	47.19	0.1271
D-2	6	46.82	0.1282
D-3	7	47.51	0.1473
D-4	7	51.53	0.1359

ca. 0.12 MPa/m.

$$T_s = \frac{P}{M - C} = \frac{5.1}{58.86 - 15.6} \approx 0.1179\ \text{MPa/m}. \quad (16)$$

The maximum water resistance coefficient of floor rock mass is equal to the critical water inrush coefficient of Ordovician limestone in coalface 1101. This means that, when the value of conventional water inrush system in coalface is greater than or equal to the maximum water resistance coefficient, the floor of coalface is predicted to be in water inrush state. When the value of conventional water inrush system is less than the maximum water resistance coefficient, the floor of coalface is predicted not to be in water inrush state.

According to the results presented in Table 7, the minimum value of the maximum water resistance coefficient of 1101 coalface floor is 0.1271 MPa/m, whereas the conventional result of 1101 coalface floor water inrush coefficient is 0.1179 MPa/m. Therefore, the value of conventional water inrush system in 1101 coalface is smaller than the maximum water resistance coefficient. It is predicted that there will be no water inrush after the reconstruction of floor strata in 1101 coalface. In addition, according to the results calculated using "coal mine water prevention and control rules" in 2019, the maximum water resistance coefficient of 1101 coalface floor is far greater than the water inrush coefficient calculated using the regulations. Therefore, the coalface meets the requirements of the specification.

4.3. Evaluation by Mine Electric Method. In the auxiliary roadway on both sides of 1101 coalface, forty measuring points were set up. Furthermore, 1440 groups of data were collected before and after the grouting using mine electrical method's quality evaluation standard "coal electrical method exploration specification" (MT/T 898-2000). The arithmetic mean square error of apparent resistivity and the mean square error of all inspection points meet the deviation standard stipulated in the specification. Additionally, the data acquisition quality of the mine electric method is excellent.

4.3.1. Analysis of the Test Data in Railway Laneway. As shown in Figure 6, the karst of Xujiazhuang limestone aquifer begins to develop before grouting. The slice of apparent resistivity value line in floor electrical exploration of 1101 working face shows that there are many abnormal areas in the Xujiazhuang limestone stratum. After the grouting, the apparent resistivity isoline profile of Xujiazhuang limestone aquifer shows that the abnormal area decreases significantly. It is mainly concentrated between the survey points No. 45-65 in the railway laneway. Herein, these areas are called abnormal areas III and IV. After the grouting transformation, the abnormal points disappeared in a large area. In most areas near the railway laneway, the effect of floor grouting reinforcement is much better.

4.3.2. Analysis of the Test Data in Belt Roadway. As mentioned earlier, limestone karst in Xujiazhuang is relatively developed. According to the isoline profile of apparent resistivity in the bottom plate of 1101 coalface, there are many abnormal regions in Xujiazhuang limestone. After the grouting transformation, the contour profile of apparent

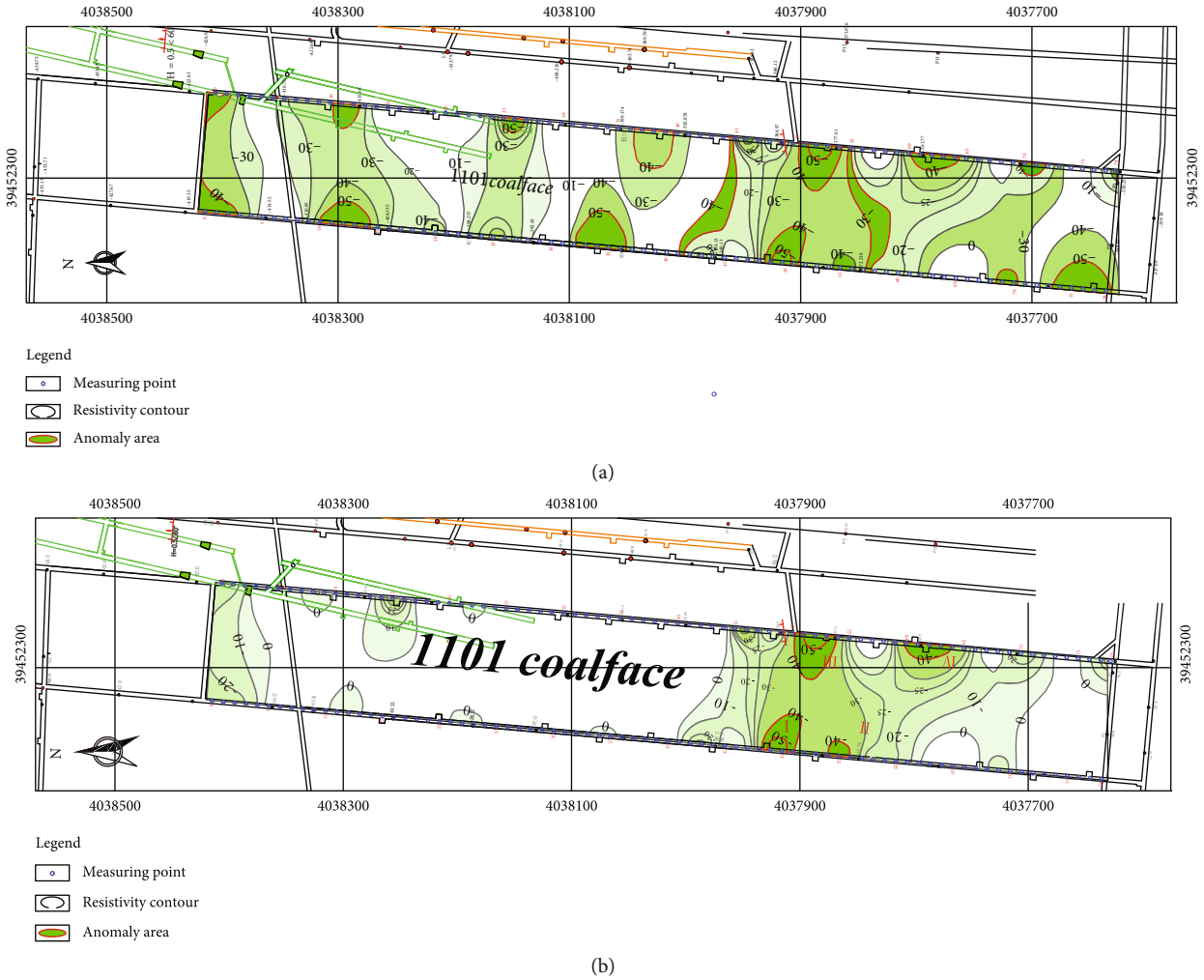

Figure 6: Isoline section of low resistivity abnormal area of Xujiazhuang limestone aquifer before and after the grouting reconstruction.

resistivity of Xujiazhuang limestone in the belt lane shows that the abnormal area is also obviously reduced. The abnormal area is mainly concentrated between the measuring points No. 45-60 in the belt roadway. Herein, these areas are called abnormal areas I and II. After the grouting transformation, the abnormal points disappeared in a large area, indicating that the grouting reinforcement effect of the floor in most areas near the belt roadway is good, though there still are some abnormal areas.

The apparent resistivity profile within 60 m of the vertical direction of the coal seam floor and the isoline slice of the apparent resistivity of grouting transformation layer is comprehensively analyzed. It can be seen that the overall effect of grouting transformation and reinforcement of Xujiazhuang limestone stratum in the floor of 1101 coalface is quite remarkable, and the effect of grouting transformation in other areas is much better except for the four abnormal areas in the middle of coalface.

4.4. Evaluation of Water Disaster Control Effect Using GIS System. According to the requirements of the above methodology, the final pressure and the degree of grouting of single-point grouting in branch bedding boreholes are analyzed. There are 297 grouting coordinate points of Xujiazhuang limestone under the floor of 1101 coalface. Firstly, the grouting pressure of each point is statistically analyzed. Secondly, the Kriging algorithm is used for interpolation calculations. Finally, the contour map of the final grouting pressure is drawn.

The hydraulic pressure of Xujiazhuang limestone aquifer is 3.35-4.40 MPa. According to the calculations, the final grouting pressure should not be less than 10 MPa, and the grout diffusion range is about 46.75 m. However, in the actual construction process, the final grouting pressure of a small number of boreholes cannot meet the requirements of design pressure. According to the previous grouting experiences, the final pressure should not be less than 8.50 MPa, which can be considered qualified grouting effect. Therefore, according to the grouting hole data of Xujiazhuang limestone stratum, the displacement data of water stress center in the observation hole of pumping test, and the final pressure of horizontal directional grouting, the grouting effect can be divided into three levels. These three levels are the divided standard zone (final pressure $\geq$ 10 MPa), the qualified zone (8.50 MPa $\leq$ final pressure $<$ 10 MPa), and the relatively weak zone (final pressure $<$ 8.50 MPa). Based on the

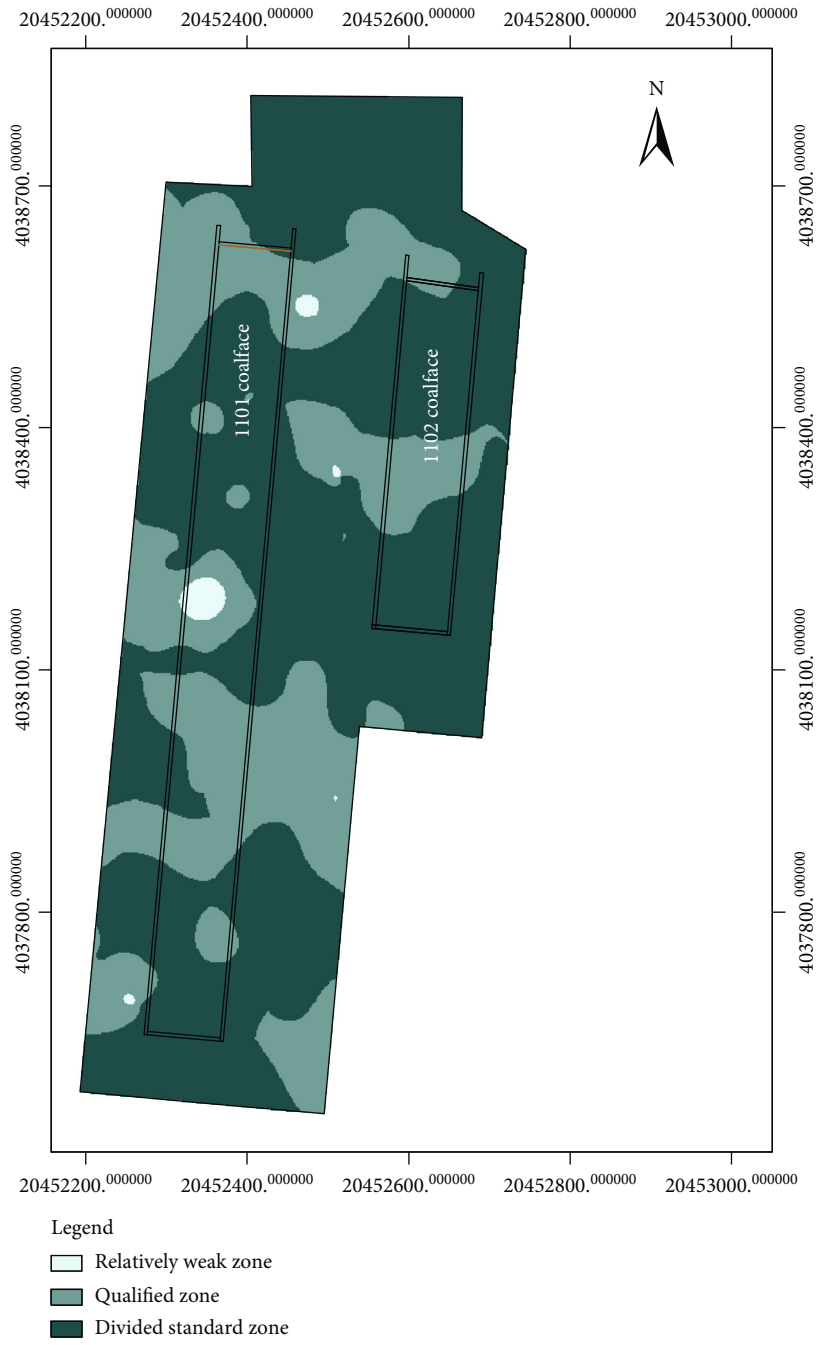

Figure 7: Evaluation of the directional drilling and grouting in Xujiazhuang limestone aquifer.

GIS system, the grouting effect of the floor of 1101 coalface is divided into several zones, and the location of weak area is comprehensively analyzed by combining the degree of grouting of the relatively weak area.

According to the final pressure and the degree of grouting of single-point grouting in horizontal directional branch drilling of Xujiazhuang limestone stratum, the evaluation and analysis of data regarding the grouting of Xujiazhuang limestone under the floor of 1101 working face are conducted (see Figure 7).

4.5. Use of Dense Boreholes for Assessment. According to the data of abnormal points and weak areas provided by the above four steps, the fifth step of the SVE method is executed. The geophysical exploration of boreholes was carried out underground. The Xujiazhuang limestone under the floor of coalface 1101 was inspected by drilling. The drilling spacing was set to be 60 m to ensure the floor area of coalface 1101 was fully covered. The anomalies and weak links in the above four steps should be carefully pointed out and addressed. A total of 216 holes were drilled in the

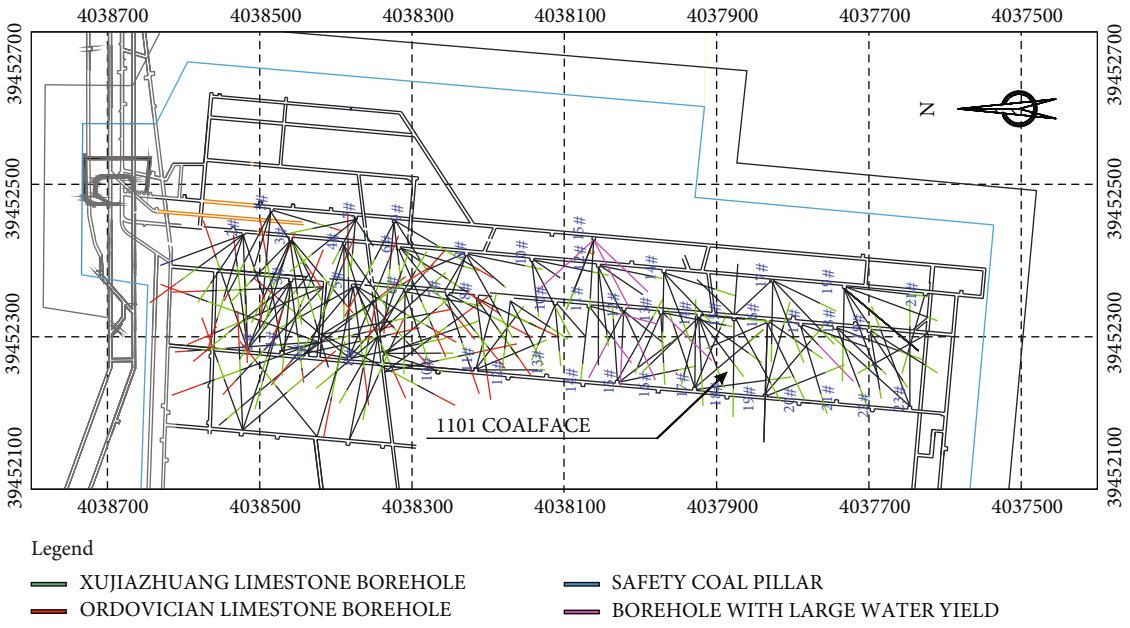

Figure 8: Layout of the inspection borehole in the Xujiazhuang limestone aquifer.

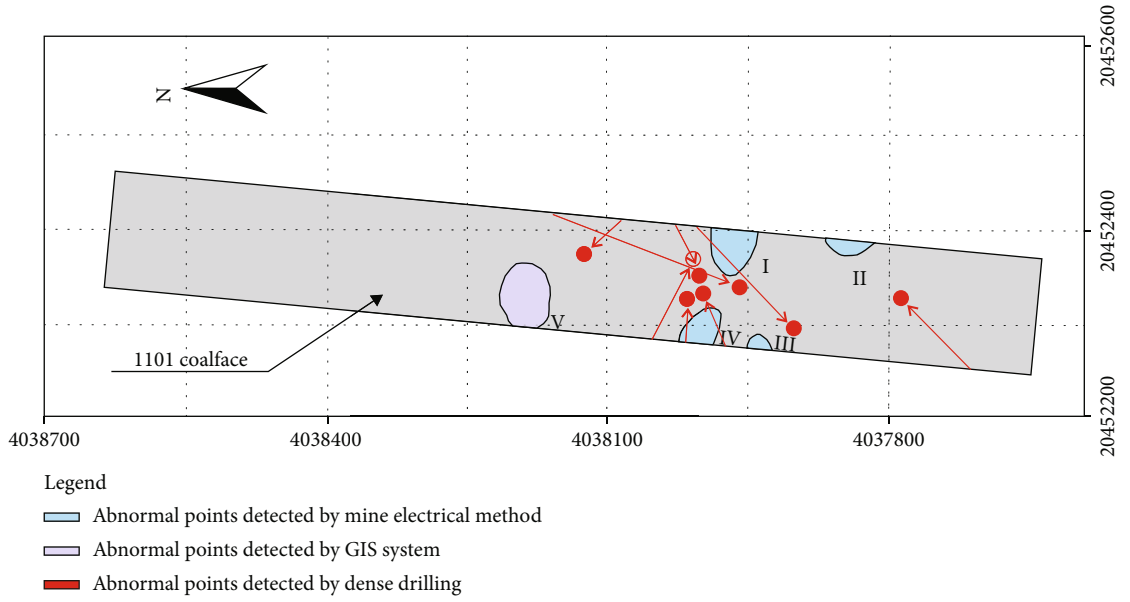

Figure 9: Evaluation chart of the floor water disaster control effect in 1101 coalface.

Xujiazhuang limestone aquifer under the floor of 1101 coalface. As shown in Figure 8, when the water inflow of a single hole is greater than 5 m^3/h, it is necessary to carry out underground slurry replenishment treatment. According to the monitoring data of the exploration holes in the mine, 97.2% of the inspection boreholes have a single-hole water inflow of less than 5 m^3/h. In addition, six inspection boreholes in Xujiazhuang limestone stratum failed to meet the set requirements, and the single-hole water inflow was found to be greater than 10 m^3/h, indicating that there is still a blind area for surface directional horizontal drilling grouting.

4.6. SVE Method. According to the technical requirements in the above methodology, the SVE method of floor water disaster control effect before mining is explained step by step from "surface to point." Firstly, the hydraulic conductivity and permeable rate of the grouting reconstruction layer are analyzed as a whole. The results show that the Xujiazhuang limestone aquifer has been transformed into micropermeable rock mass with good water resistance after the floor grouting transformation of 1101 coalface. Secondly, the overall analysis of the water blocking ability of the reformed layer is conducted. The results show that the conventional water inrush coefficient of 1101 coalface is less than the

maximum water resistance coefficient. Additionally, it is predicted that the floor of 1101 coalface would not undergo water inrush after reconstruction.

Thirdly, the analysis and evaluation are carried out by using the mine electrical detection method. Many detection points are set up in the auxiliary roadway of the coalface for monitoring. Comparing the apparent resistivity isoline map before and after the grouting transformation, four abnormal points after high-pressure grouting on the ground were determined. Fourthly, according to the evaluation of the effect of grouting using the GIS system, the relatively weak area after high-pressure grouting on the ground was delineated. According to the abovementioned four steps of the SVE method, the abnormal points and weak areas of Xujiazhuang limestone aquifer under the floor of 1101 coalface after high-pressure grouting were determined.

The fifth step is to use the dense detection boreholes to carry out comprehensive detection underground, as shown in Figure 8. This is done to delimit the weak area of the coal seam floor water disaster control effect. The weak areas found in the previous four steps are mainly detected. Finally, a five-step evaluation method is formed. The first two steps include qualitative evaluation, while the last three involve quantitative evaluations (Figure 9).

4.7. Supplementary Grouting in Underground. Underground supplementary grouting was carried out in 6 drilling areas where the water inflow of a single hole was more than $5\,m^3/h$ from the bottom plate of 1101 coalface. After the grouting requirements are met, another test hole shall be constructed within 5 m of the hole until the water inflow of a single hole is less than $5\,m^3/h$. According to the data provided by the mining company, the water inflow of single hole of the above six measuring points is found to be less than $5\,m^3/h$ after the underground supplementary grouting reconstruction.

Therefore, it is inferred that the floor grouting transformation of 1101 coalface basically meets the design requirements. In order to make sure that all inspection boreholes meet the requirements of safe design and sufficient protection, the trial mining work can be carried out on 1101 coalface.

At the end of November 2019, the mining of the whole coalface 1101 was finished, and the mining effect was good. The obtained results show that the roof water inflow was less than $8\,m^3/h$, while the floor ash water inflow was less than $27\,m^3/h$. Furthermore, the overall water inflow of 1101 coalface was less than $35\,m^3/h$.

5. Conclusions

In this paper, a scientific and systematic study is conducted on the evaluation of prevention and control effect of water inrush disaster in the floor of deep coal seam mining. Based upon the results, the following conclusions are drawn:

(1) For the very first time, the SVE method is proposed for the prevention and control effect of water inrush disaster in the deep coal seam floor. The method considers factors, such as hydraulic conductivity, permeable rate, and water-resisting ability of effective water resisting layer of coal seam floor after prevention and control. Combined with methods such as in situ test of the mine electrical method, GIS analysis of grouting data, and layout detection of dense boreholes, a comprehensive sequence verification and evaluation system for grouting transformation area of coal seam floor was formed

(2) The core of the SVE system is the data integration analysis based on GIS and the synergistic mechanism of each evaluation unit. The proposed method can scientifically and effectively evaluate the prevention and control effect of water inrush disaster in deep mining

(3) The proposed SVE method should be used for reference to other coal mining areas. The scientific effectiveness of the evaluation method shall be further monitored after acquiring more practical data and experience

Data Availability

The data used to support the findings of this study are available from the authors upon request.

Conflicts of Interest

The authors declare that they have no conflicts of interest.

Acknowledgments

This work was supported by the Natural Science Foundation of Jiangsu Province under Grant Nos. BK20190646 and BK20221319.

References

[1] X. Chen, L. Li, L. Wang, and L. Qi, "The current situation and prevention and control countermeasures for typical dynamic disasters in kilometer-deep mines in China," *Safety Science*, vol. 115, pp. 229–236, 2019.

[2] X. Y. Qu, L. Q. Shi, W. F. Gao, and M. Qiu, "Characteristics of faults in the Liangzhuang mining area and their control on karst development in Ordovician limestones," *Carbonates and Evaporites*, vol. 35, no. 4, pp. 1–4, 2020.

[3] S. Qu, G. Wang, Z. Shi, P. Zhou, Q. Xu, and Z. Zhu, "Temporal changes of hydraulic properties of overburden aquifer induced by longwall mining in ningtiaota coalfield, Northwest China," *Journal of Hydrology*, vol. 582, article 124525, 2020.

[4] S. Liu, Y. Fei, Y. Xu, L. Huang, and W. Guo, "Full-floor grouting reinforcement for working faces with large mining heights and high water pressure: a case study in China," *Mine Water and the Environment*, vol. 39, no. 2, pp. 268–279, 2020.

[5] Y. L. Xu, K. R. Pan, and H. Zhang, "Investigation of key techniques on floor roadway support under the impacts of superimposed mining: theoretical analysis and field study," *Environmental Earth Sciences*, vol. 78, no. 15, pp. 1–4, 2019.

[6] J. C. Zhang, "Investigations of water inrushes from aquifers under coal seams," *International Journal of Rock Mechanics and Mining Sciences*, vol. 42, no. 3, pp. 350–360, 2005.

[7] W. F. Gao, P. H. Zhai, L. L. Xiao, and T. H. Liu, "Research and application of the 3D DC resistivity method with around working face," *Chinese Journal of Geophysics*, vol. 63, no. 9, pp. 3534–3544, 2020.

[8] Q. Wu, Y. Z. Du, H. Xu, Y. W. Zhao, X. Y. Zhang, and Y. Yao, "Finding the earliest arrival path through a time-varying network for evacuation planning of mine water inrush," *Safety Science*, vol. 130, article 104836, 2020.

[9] M. Y. Khan, G. Q. Xue, W. Y. Chen, and C. D. Boateng, "Investigation of groundwater in-rush zone using petrophysical logs and short-offset transient electromagnetic (sotem) data," *Journal of Environmental and Engineering Geophysics*, vol. 25, no. 3, pp. 433–437, 2020.

[10] W. H. Shi and T. H. Yang, "A coupled nonlinear flow model for particle migration and seepage properties of water inrush through broken rock mass," *Geofluids*, vol. 2020, Article ID 1230542, 14 pages, 2020.

[11] L. L. Xiao, Q. Wu, C. Niu et al., "Application of a new evaluation method for floor water inrush risk from the Ordovician fissure confined aquifer in Xiayukou coal mine, Shanxi, China," *Carbonates and Evaporites*, vol. 35, no. 3, p. article 97, 2020.

[12] J. W. Bai, Z. J. Zhu, R. T. Liu, M. Wang, Q. S. Zhang, and M. Heng, "Groundwater runoff pattern and keyhole grouting method in deep mines," *Bulletin of Engineering Geology and the Environment*, vol. 80, no. 7, pp. 5743–5755, 2021.

[13] S. N. Dong, H. Wang, X. M. Guo, and Z. F. Zhou, "Characteristics of water hazards in China's coal mines: a review," *Mine Water and the Environment*, vol. 40, no. 2, pp. 325–333, 2021.

[14] P. Buklwski, "Water Hazard assessment in active shafts in upper Silesian Coal Basin mines," *Mine Water and the Environment.*, vol. 30, no. 4, pp. 302–311, 2011.

[15] C. S. Wang, Y. J. Sun, and Y. Hang, "Application of fault tree analysis to risk assessment of potential water-inrush hazards in coal mining," *Chinese Journal of Rock Mechanics and Engineering*, vol. 28, no. 2, pp. 298–305, 2009.

[16] Z. Rezaei and M. Ataee-pour, "Assessment of mine water environmental impact: a fuzzy reliability approach," *Mine Water and the Environment*, vol. 38, no. 1, pp. 30–38, 2019.

[17] B. Fang, "Method for quickly identifying mine water inrush using convolutional neural network in coal mine safety mining," *Wireless Personal Communication*, vol. 2021, pp. 1–18, 2021.

[18] S. C. Zhang, B. T. Shen, X. G. Zhang, Y. Y. Li, W. B. Sun, and J. H. Zhao, "Modelling the coupled fracture propagation and fluid flow in jointed rock mass using FRACOD," *Geomechanics and Engineering*, vol. 22, no. 6, pp. 529–540, 2020.

[19] W. R. D. Wilson and S. M. Mahdavian, "A thermal Reynolds equation and its application in the analysis of plasto-hydrodynamic inlet zones," *Journal of Lubrication Technology*, vol. 96, no. 4, pp. 572–577, 1974.

[20] R. Mollehuara-Canales, E. Kozlovskaya, J. P. Lunkka, H. Guan, and K. Moisio, "Geoelectric interpretation of petrophysical and hydrogeological parameters in reclaimed mine tailings areas," *Journal of Applied Geophysics*, vol. 181, article 104139, 2020.